27
9-21-81

B1203

①

242 NTIS

MASTER

UCID-19185

A SUMMARY OF THE LLNL ONE-DIMENSIONAL TRANSPORT-KINETICS MODEL OF THE TROPOSPHERE AND STRATOSPHERE: 1981

D. J. Wuebbles

September, 1981

Lawrence Livermore Laboratory

Work performed under the auspices of the U.S. Department of Energy by the Lawrence Livermore Laboratory under Contract W-7405-Eng-48.

UCID-19185

A SUMMARY OF
THE LLNL ONE-DIMENSIONAL TRANSPORT-KINETICS
MODEL OF THE TROPOSPHERE AND STRATOSPHERE: 1981

D. J. Wuebbles

September, 1981

Since the LLNL one-dimensional coupled transport and chemical kinetics model of the troposphere and stratosphere was originally developed in 1972 (Chang et al., 1974), there have been many changes to the model's representation of atmospheric physical and chemical processes. The purpose this report is to provide a brief description of the current LLNL one-dimensional coupled transport and chemical kinetics model of the troposphere and stratosphere.

Model Structure:

The LLNL 1-D model currently extends from the ground to 56.25 km. The vertical grid structure is variable, but usually has a 0.5-km-thick layer at the surface, 1-km thick layers extending from 0.5 to 34.5 km, a 1.75-km thick layer between 34.5 and 36.25 km and 2.5 km thick layers extending to 56.25 km.

Work performed under the auspices of the U.S. Department of Energy by the Lawrence Livermore National Laboratory under contract W-7405-Eng-48.

Three of the minor constituents, $O(^1D)$, H, and N in the model are assumed to be in instantaneous equilibrium. Each of the other 44 species in the model has its concentration calculated at each of 44 vertical levels extending from the surface to 56.25 km. There is a continuity equation describing the time rate of change of each of the 44 minor constituents at each altitude. The numerical technique used to solve the set of approximately 2000 differential equations (resulting from a continuity equation for each species at each grid level) is the GEAR method as described by Chang et al. (1974). The main advantage of this method, which is a variable order, multistep, implicit method, is its ability to solve sets of mathematically stiff differential equations for almost any set of input parameters, initial and boundary conditions, in particular those resulting from the chemical kinetics system.

TRANSPORT PARAMETERIZATION

The transport of atmospheric trace constituents in the 1-D model, is an empirical representation not utilizing observed atmospheric motion directly but rather is based on the observations of the temporal and spatial distributions of selected trace species. In the LLNL one-dimensional model, the K_z profile was originally based on an analysis of CH_4 and N_2O measurements (Chang in NRC, 1976) with consideration also given to measurements of radionuclide debris transport in the lower stratosphere. This K_z profile is shown in Figure 1. Although this K_z profile is used in most model calculations, other K_z representations, such as those used in other models may be used as well. Several K_z profiles have been used to test the sensitivity of calculated results to transport parameterization uncertainties (Chang, 1974; Duewer et al., 1977; Luther et al., 1979).

Chemical Kinetics System

The LLNL 1-D model presently contains 141 chemical and photochemical reactions to determine the concentrations of 47 minor atmospheric constituents. These constituents include all of the known odd oxygen (O_x), odd hydrogen (HO_x), odd chlorine ($C\ell O_x$), and odd nitrogen (NO_x) species important to tropospheric and stratospheric chemistry. Also included are source species (N_2O, H_2O, chlorocarbons), plus all of the species resulting from methane oxidation. The chemistry of several other species, such as C_2H_4 and C_2H_6, have also been studied with the model, but are not included here. Sulfur chemistry will be added to the model in the near future for studying the stratospheric aerosol layer.

The chemistry used currently in the model is primarily that recommended by the joint meeting of the NASA Panel for Data Evaluation and the CODATA Task Group on Chemical Kinetics in March, 1981 (W. Demore, private communication, 1981). Tables 1 through 3 show the reactions and rates currently in the model. For the photodissociation reactions (Table 3), the sources of the absorption cross-sections and quantum yields used in the model to compute photodissociation rates are shown. Several reactions are included that are not given in the NASA-CODATA recommendations. These reactions mostly involve chlorocarbons whose rates have been measured (but not considered in the NASA-CODATA recommendation) or for which reasonable estimates of the reaction rate can be made. There are also several reactions included for which rate estimates are made based on similar corresponding reactions.

The model is programmed such that any chemical rate can easily be modified. This ability is extremely useful in testing the effect of new laboratory measurements or studying the effect of reaction rate uncertainties. For example, the previous NASA Panel recommendations (NASA Panel for Data Evaluation, 1981) gave two possible rates for $C\ell ONO_2$ (chlorine nitrate) production. The faster of these rates is based on the rate of $C\ell O + NO_2$ in laboratory studies, while the slower rate reflects the possibility, also based on laboratory studies, that chlorine nitrate isomers are being formed as well as $C\ell ONO_2$. These isomers are assumed to dissociate immediately. In the model, the slower rate is used, as recommended by the combined NASA-CODATA Panels. However, it is straightforward to test the sensitivity of the model to the faster rate as well.

TABLE 1. Chemical reactions and rate coefficients where $k = Ae^{B/T}$ used in the 1981 model chemistry.

	Reaction	A	B	Note
1.	$O + O_2 + M \rightarrow O_3 + M$	see Table 2		3
2.	$O + O_3 \rightarrow 2O_2$	1.5×10^{-11}	-2218	1
3.	$O_3 + NO \rightarrow NO_2 + O_2$	3.8×10^{-12}	-1580	1
4.	$O + NO_2 \rightarrow NO + O_2$	9.3×10^{-12}	0	1
5.	$N_2O + O(^1D) \rightarrow N_2 + O_2$	4.4×10^{-11}	0	1
6.	$N_2O + O(^1D) \rightarrow 2NO$	7.2×10^{-11}	0	1
7.	$N + O_2 \rightarrow NO + O$	4.4×10^{-12}	-3220	1
8.	$N + NO \rightarrow N_2 + O$	3.4×10^{-11}	0	1
9.	$O(^1D) + H_2O \rightarrow 2OH$	2.3×10^{-10}	0	1
10.	$O_3 + OH \rightarrow HO_2 + O_2$	1.6×10^{-12}	-940	1
11.	$O + OH \rightarrow O_2 + H$	2.3×10^{-11}	+110	1
12.	$O_3 + HO_2 \rightarrow OH + 2O_2$	1.4×10^{-14}	-580	1
13.	$O + HO_2 \rightarrow OH + O_2$	3.5×10^{-11}	0	1
14.	$H + O_2 + M \rightarrow HO_2 + M$	see Table 2		3
15.	$O_3 + H \rightarrow OH + O_2$	1.4×10^{-10}	-470	1
16.	$HO_2 + HO_2 \rightarrow H_2O_2 + O_2$	3.0×10^{-12}	0	1
17.	$HO_2 + OH \rightarrow H_2O + O_2$	8.0×10^{-11}	0	1
18.	$OH + NO_2 + M \rightarrow HNO_3 + M$	see Table 2	1	
19	$OH + HNO_3 \rightarrow H_2O + NO_3$	1.52×10^{-13}	+649	1,10
20.	$H_2O_2 + OH \rightarrow H_2O + HO_2$	2.9×10^{-12}	-160	1
21.	$N_2 + O(^1D) + M \rightarrow N_2O + M$	see Table 2		3
22.	$N + NO_2 \rightarrow N_2O + O$	2.1×10^{-11}	-800	2
23.	$NO + O + M \rightarrow NO_2 + M$	see Table 2		3
24.	$NO + HO_2 \rightarrow NO_2 + OH$	3.7×10^{-12}	+240	1
25.	$H_2 + O(^1D) \rightarrow OH + H$	1.1×10^{-10}	0	1
26.	$OH + OH \rightarrow H_2O + O$	4.5×10^{-12}	-275	1
27.	$N + O_3 \rightarrow NO + O_2$	2.0×10^{-11}	-3000	4
28.	$NO_2 + O_3 \rightarrow NO_3 + O_2$	1.2×10^{-13}	-2450	1

TABLE 1. Continued

	Reaction	A	B	Note
29.	$OH + OH + M \rightarrow H_2O_2 + M$	see Table 2		3
30.	$H_2O_2 + O \rightarrow OH + HO_2$	1.0×10^{-11}	-2500	1
31.	$CO + OH + M \rightarrow H + CO_2 + M$	see Table 2		3
32.	$O(^1D) + M \rightarrow O + M$	2.1×10^{-11}	99	5
33.	$C\ell + O_3 \rightarrow C\ell O + O_2$	2.8×10^{-11}	-257	1
34.	$C\ell + NO_2 + M \rightarrow C\ell NO_2 + M$	see Table 2		3
35.	$C\ell O + O \rightarrow C\ell + O_2$	7.7×10^{-11}	-130	1
36.	$NO + C\ell O \rightarrow NO_2 + C\ell$	6.2×10^{-12}	294	1
37.	$C\ell O + NO_2 + M \rightarrow C\ell ONO_2 + M$	see Table 2		3
38.	$HC\ell + O(^1D) \rightarrow C\ell + OH$	1.4×10^{-10}	0	1
39.	$OH + HC\ell \rightarrow H_2O + C\ell$	2.8×10^{-12}	-425	1
40.	$O + HC\ell \rightarrow OH + C\ell$	1.14×10^{-11}	-3370	1
41.	$C\ell + HO_2 \rightarrow HC\ell + O_2$	4.8×10^{-11}	0	1
42.	$CFC\ell_3 + O(^1D) \rightarrow 3C\ell$	2.2×10^{-10}	0	1,6
43.	$CF_2C\ell_2 + O(^1D) \rightarrow 2C\ell$	1.4×10^{-10}	0	1,6
44.	$C\ell + H_2 \rightarrow HC\ell + H$	3.5×10^{-11}	-2290	1
45.	$C\ell + H_2O_2 \rightarrow HC\ell + HO_2$	1.1×10^{-11}	-980	1
46.	$C\ell ONO_2 + O \rightarrow C\ell O + NO_3$	3.0×10^{-12}	-808	1,10
47.	$CH_3C\ell + OH \rightarrow C\ell + H_2O + HO_2$	1.8×10^{-12}	-1112	1,6
48.	$NO + NO_3 \rightarrow 2NO_2$	2.0×10^{-11}	0	1
49.	$NO_2 + O + M \rightarrow NO_3 + M$	see Table 2		3
50.	$NO_2 + NO_3 + M \rightarrow N_2O_5 + M$	see Table 2		3
51.	$N_2O_5 + M \rightarrow NO_2 + NO_3 + M$	see Table 2		3
52.	$N_2O_5 + H_2O \rightarrow 2HNO_3$	5.0×10^{-22}	0	7
53.	$O(^1D) + O_3 \rightarrow 2O_2$	1.2×10^{-10}	0	1
54.	$HO_2 + HO_2 + H_2O \rightarrow H_2O_2 + O_2 + H_2O$	see Table 2		3
55.	$O + NO_3 \rightarrow O_2 + NO_2$	1.0×10^{-11}	0	1
56.	$HO_2 + NO_2 + M \rightarrow HNO_4 + M$	see Table 2		3
57.	$HNO_4 + M \rightarrow HO_2 + NO_2 + M$	see Table 2		3
58.	$OH + HNO_4 \rightarrow H_2O + NO_2 + O_2$	4.0×10^{-12}	0	1,10
59.	$C\ell + HNO_4 \rightarrow HC\ell + NO_2 + O_2$	3.0×10^{-12}	-300	8
60.	$HO_2 + C\ell O \rightarrow O_2 + HOC\ell$	4.6×10^{-13}	710	1
61.	$C\ell + HOC\ell \rightarrow HC\ell + C\ell O$	3.0×10^{-12}	-300	8

TABLE 1. Continued

	Reaction	A	B	Note
62.	$OH + HOC\ell \rightarrow H_2O + C\ell O$	3.0×10^{-12}	-150	1
63.	$O + HOC\ell \rightarrow OH + C\ell O$	1.0×10^{-11}	-2200	1
64.	$OH + CH_4 \rightarrow CH_3 + H_2O$	2.4×10^{-12}	-1710	1
65.	$O + CH_4 \rightarrow CH_3 + OH$	3.5×10^{-11}	-4550	1
66.	$O(^1D) + CH_4 \rightarrow CH_2O + H_2$	1.5×10^{-11}	0	1
67.	$O(^1D) + CH_4 \rightarrow CH_3 + OH$	1.4×10^{-10}	0	1
68.	$CH_4 + C\ell \rightarrow HC\ell + CH_3$	9.6×10^{-12}	-1350	1
69.	$C\ell + CH_3C\ell \rightarrow HO_2 + CO + 2HC\ell$	3.4×10^{-11}	-1260	1,6
70.	$CH_3O_2 + NO \rightarrow NO_2 + CH_3O$	7.4×10^{-12}	0	1
71.	$C\ell + CH_2O \rightarrow HC\ell + HCO$	8.2×10^{-11}	-34	1
72.	$CH_3O_2 + HO_2 \rightarrow CH_3OOH + O_2$	6.0×10^{-14}	0	1
73.	$CH_3O + O_2 \rightarrow CH_2O + HO_2$	1.0×10^{-12}	-2050	1
74.	$OH + CH_2O \rightarrow H_2O + HCO$	1.0×10^{-11}	0	1
75.	$O + CH_2O \rightarrow HCO + OH$	3.0×10^{-11}	-1550	1,10
76.	$HCO + O_2 \rightarrow CO + HO_2$	5.0×10^{-12}	0	1
77.	$OH + CH_3OOH \rightarrow CH_3O_2 + H_2O$	2.2×10^{-12}	-160	1,10
78.	$CH_3 + O \rightarrow CH_2O + H$	1.3×10^{-10}	0	1
79.	$CH_3O_2 + O_3 \rightarrow CH_3O + 2O_2$	1.0×10^{-14}	-600	9
80.	$CH_3O_2 + O \rightarrow CH_3O + O_2$	3.0×10^{-11}	0	9
81.	$C\ell O + OH \rightarrow HO_2 + C\ell$	9.1×10^{-12}	0	1,10
82.	$CH_3 + O_2 + M \rightarrow CH_3O_2 + M$	see Table 2		3
83.	$C\ell O + OH \rightarrow HC\ell + O_2$	Not used ($\sim 10^{-22}$)		
84.	$H_2 + OH \rightarrow H_2O + H$	7.7×10^{-12}	-2100	1
85.	$H + HO_2 \rightarrow H_2 + O_2$	4.2×10^{-11}	-350	12
86.	$OH + CH_3OOH \rightarrow CH_2O + H_2O + OH$	5.0×10^{-12}	-750	1,10
87.	$O + HNO_4 \rightarrow OH + NO_2 + O_2$	7.4×10^{-12}	-2630	1,10
88.	$OH + C\ell ONO_2 \rightarrow HOC\ell + NO_3$	1.2×10^{-12}	-333	1,10
89.	$C\ell + C\ell ONO_2 \rightarrow 2C\ell + NO_3$	1.7×10^{-12}	-607	1,10
90.	$HONO + OH \rightarrow H_2O + NO_2$	6.6×10^{-12}	0	12
91.	$OH + NO + M \rightarrow HONO + M$	see Table 2		3
92.	$O + OC\ell O \rightarrow C\ell O + O_2$	2.5×10^{-11}	-1166	1
93.	$NO + OC\ell O \rightarrow NO_2 + C\ell O$	2.5×10^{-12}	-600	1

TABLE 1. Continued

	Reaction	A	B	Note
94.	$OH + CH_3CC\ell_3 \rightarrow H_2O + 3C\ell$	5.4×10^{-12}	-1820	1,6
95.	$OH + CFC\text{-}21 \rightarrow 2C\ell$	8.9×10^{-13}	-1013	1,6
96.	$O(^1D) + CFC\text{-}13 \rightarrow C\ell$	1.0×10^{-10}	0	11
97.	$O(^1D) + CFC\text{-}112 \rightarrow 4C\ell$	3.0×10^{-10}	0	11
98.	$OH + CFC\text{-}142b \rightarrow C\ell$	1.5×10^{-12}	-1800	12
99.	$O(^1D) + CFC\text{-}113 \rightarrow 3C\ell$	2.75×10^{-10}	0	13
100.	$O(^1D) + CFC\text{-}114 \rightarrow 2C\ell$	1.62×10^{-10}	0	13
101.	$O(^1D) + CFC\text{-}115 \rightarrow C\ell$	1.00×10^{-10}	0	14
102.	$OH + CFC\text{-}22 \rightarrow H_2O + C\ell$	7.8×10^{-13}	-1530	1,6
103.	$O(^1D) + CC\ell_4 \rightarrow 4C\ell$	3.5×10^{-10}	0	1,6

NOTES TO TABLE 1

1. Draft report of the joint meeting of the NASA Panel for Data Evaluation and the CODATA Task Group on Chemical Kinetics (W. DeMore, private communication, 1981).

2. NASA Panel for Data Evaluation (JPL 81-3), 1981.

3. The reaction is pressure dependent. See Table A-2 for discussion.

4. Estimate designed to be compatible with upper limit given in reference 1, and low enough to have no significant effect on model performance. Reaction is retained only to facilitate reintroduction if the evaluated upper limit should prove to be in error.

5. Weighted average of the rates of $O(^1D)$ + N_2 and $O(^1D)$ + O_2 from reference 1.

6. Product chemistry has been simplified.

7. Estimated reaction rate. This estimate is designed to include a possible heterogeneous contribution to the overall reaction. Important only in the lower troposphere.

8. Estimated reaction rate. This rate is estimated based on the assumption that HNO_4 and $HOC\ell$ resemble H_2O_2 (as treated in JPL, 1979) in reactions with $C\ell$ and OH.

9. Estimated reaction rate. Rate is estimated based on the assumption that CH_3O_2 closely resembles HO_2 in reaction with O or O_3.

10. Products are not given in references 1 or 2. The assumed products are based on products that seem the most chemically plausible.

11. Based on formula given in Davidson et al., (1978).

12. Hampson (1980).

13. Pitts et al. (1974).

14. Estimate based on consideration of reaction rate of other molecules with $O(^1D)$.

15. CFC-21 = $CHF C\ell_2$
    CFC-22 = $CH F_2 C\ell$
    CFC-13 = $C C\ell F_3$
    CFC-112 = $CFC\ell_2 CF C\ell_2$
    CFC-142b = $CH_3C C\ell F_2$
    CFC-113 = $CFC\ell_2 CF_2C\ell$
    CFC-114 = $CF_2 C\ell CF_2 C\ell$
    CFC-115 = $CF_2 C\ell CF_3$

TABLE 2. Rate coefficients used for pressure-dependent reactions.

Expression 1:

$$k = \frac{A_o[M](300/T)^{n_o}}{1 + A_o[M](300/T)^{n_o}/A_i(300/T)^{n_i}} \quad 0.6^{1/D}, \quad D = 1 + \left\{\log_{10} \frac{A_o[M](300/T)^{n_o}}{A_i(300/T)^{n_i}}\right\}^2$$

Reaction	A_o	n_o	A_i	n_i	Note
$HO_2 + NO_2 + M \rightarrow HNO_4 + M$	2.1×10^{-31}	5.0	6.5×10^{-12}	2.0	1
$OH + NO_2 + M \rightarrow HNO_3 + M$	2.6×10^{-30}	2.9	2.4×10^{-11}	1.3	1
$Cl O + NO_2 + M \rightarrow Cl ONO_2 + M$	4.5×10^{-32}	3.8	1.5×10^{-11}	1.9	1,2
$O + O_2 + M \rightarrow O_3 + M$	1.6×10^{-31}	3.4	1.5×10^{-11}	1.9	1,2
	6.2×10^{-34}	2.1	---	--	1
$CH_3 + O_2 + M \rightarrow CH_3O_2 + M$	2.2×10^{-31}	2.2	2.0×10^{-12}	1.7	1
$O(^1D) + N_2 + M \rightarrow N_2O + M$	3.5×10^{-37}	0.45	---	--	1
$Cl + NO_2 + M \rightarrow Cl NO_2$	1.6×10^{-30}	1.9	3.0×10^{-11}	1.0	1
$H + O_2 + M \rightarrow HO_2 + M$	5.5×10^{-32}	1.4	---	--	1
$OH + NO + M \rightarrow HNO_2 + M$	6.7×10^{-31}	3.3	3.0×10^{-11}	1.0	1
$OH + OH + M \rightarrow H_2O_2 + M$	2.5×10^{-31}	0.8	3.0×10^{-11}	1.0	1
$NO_2 + NO_3 + M \rightarrow N_2O_5 + M$	1.4×10^{-30}	2.8	8.0×10^{-13}	0	1
$O + NO + M \rightarrow NO_2 + M$	1.2×10^{-31}	1.8	3.0×10^{-11}	0	1
$O + NO_2 + M \rightarrow NO_3 + M$	9.0×10^{-32}	2.0	2.2×10^{-11}	0	1
$N_2O_5 + M \rightarrow NO_2 + NO_3 + M$	$1.18\times10^{-3}e^{-11180/T}$	2.8	$7.52\times10^{14}e^{-11180/T}$	-0.8	3

TABLE 2. (Continued.)

		Notes
$HNO_4 + M \rightarrow HO_2 + NO_2 + M$	$k = \frac{5.2 \times 10^{-6} e^{-10015/T}}{1 + 4.86 \times 10^{-12} M^{0.61}}$	5
$OH + CO + M \rightarrow H + CO_2 + M$	$k = 1.35 \times 10^{-13} \left(1 + \frac{M}{2.46 \times 10^{+19}}\right)$	1
$HO_2 + HO_2 + H_2O \rightarrow H_2O_2 + H_2O + O_2$	$k = \frac{1.1 \times 10^{-34} e^{+3730/T}}{1 + M \times 3.5 \times 10^{-16} e^{-2060/T}}$	4

NOTES TO TABLE 2

1. Draft report for joint meeting of NASA Panel for Data Evaluation and CODATA Task Group on Chemical Kinetics, 1981.

2. Top expression is recommended in 1. The upper one is used in most of the LLNL one-dimensional calculations but because uncertainty still large, second expression is also often used.

3. Based on data in referenee 1 and the equilibrium constant from NBS 513 (1978).

4. Based on Cox (1978).

5. Based on Graham et al. (1978).

TABLE 3. Photolysis reactions. Alternative products of reaction are shown in parentheses, but they are not used in the 1981 chemistry.

	Reaction	Note
1.	$O_2 \rightarrow 2O$	1,2
2.	$O_3 \rightarrow O + O_2$	1,3
3.	$O_3 \rightarrow O(^1D) + O_2$	1,3
4.	$NO_2 \rightarrow NO + O$	1,4
5.	$N_2O \rightarrow N_2 + O(^1D)$	4
6.	$NO \rightarrow N + O$	5
7.	$HNO_3 \rightarrow OH + NO_2$	4
8.	$H_2O_2 \rightarrow 2OH$	4
9.	$HO_2 \rightarrow OH + O$	4
10.	$C\ell ONO_2 \rightarrow C\ell + NO_3$ $(C\ell O + NO_2)$	4,6
11.	$HC\ell \rightarrow H + C\ell$	4
12.	$C\ell O \rightarrow C\ell + O$	7
13.	$C\ell O \rightarrow C\ell + O(^1D)$	Not used
14.	$C\ell NO_2 \rightarrow C\ell + NO_2$	4
15.	$OC\ell O \rightarrow C\ell O + O$	7
16.	$CF_2C\ell_2 \rightarrow 2C\ell$	4,8
17.	$CFC\ell_3 \rightarrow 3C\ell$	4,8
18.	$CC\ell_4 \rightarrow 4C\ell$	4,8
19.	$N_2O_5 \rightarrow NO_3 + NO_2$ $(2NO_2 + O)$	4,6
20.	$NO_3 \rightarrow NO + O_2$	4
21.	$NO_3 \rightarrow NO_2 + O$	4
22.	$H_2O \rightarrow H + OH$	9
23.	$HNO_4 \rightarrow HO + NO_3$ $(HO_2 + NO_2)$	10,6
24.	$HOC\ell \rightarrow OH + C\ell$	4
25.	$CH_3OOH \rightarrow CH_3 + OH$	4
26.	$CH_2O \rightarrow HCO + H$	11
27.	$CH_2O \rightarrow CO + H_2$	11
28.	$CH_3C\ell \rightarrow CH_3 + C\ell$	4
29.	$HONO \rightarrow OH + NO$	4
30.	$CH_3CC\ell_3 \rightarrow 3C\ell$	4,8
31.	CFC-21 $\rightarrow 2C\ell$	4
32.	CFC-13 $\rightarrow C\ell$	13
33.	CFC-112 $\rightarrow 4C\ell$	12

Table 3. Continued

	Reaction	Note
34.	CFC-142b → Cℓ	14
35.	CFC-113 → 3Cℓ	12
36.	CFC-114 → 2Cℓ	12
37.	CFC-115 → Cℓ	12
38.	CFC-22 → Cℓ	4

NOTES FOR TABLE 3.

1. Contributes to the optical depth of the model atmosphere.

2. The Schumann-Runge bands are given a special treatment based on Hudson and Mahle (1972).

3. The quantum yields of reactions 2 and 3 are given a special treatment based on the temperature-dependent treatment of NASA Panel for Data Evaluation (1981).

4. Based on the data of NASA Panel for Data Evaluation (1981). Where data for several temperatures are given, we have used the data at ∿ 230 K.

5. Nitric oxide photolysis is based on the treatment of Frederick and Hudson (1979). We have averaged rates over the sunlit hemisphere for daytime photolysis.

6. The products used for XNO_3 (X = $C\ell$, OH, NO_2) are all based on analogy with $C\ell ONO_2$ data of Chang et al. (1979). This treatment is highly uncertain.

7. Based on data in Watson (1974).

8. Product chemistry has been simplified.

9. Treatment based on Thompson et al. (1963).

10. Treatment based on Molina and Molina (1980).

11. Treatment based on cross sections of Bass et al. (1980), quantum yields based on DeGraff and Calvert (1976) and Moortgat and Warneck (1979).

12. Based on recommendation of NASA Panel on Laboratory Measurements in NASA Reference Publication 1049 (Hudson and Reed, 1979).

13. Based on Hubrich, et al., (1977).

14. Based on Hubrich and Stuhl (1980).

Radiative Processes

Photodissociation processes in the atmosphere are often extremely important mechanisms for the production and destruction of chemical species. In the LLNL model, the rates of 38 photodissociation reactions (see Table 3) are updated as a function of altitude at each time step for all model calculations. It is necessary to continually update the photodissociation rates in order to properly account for changes in photodissociation with changes in the distribution of important absorbers of solar wavelengths such as the species O_3, CO_2 and NO_2.

There is evidence for a moderate temperature dependence in many photoabsorption cross-sections. With the exception of O_3, CH_2O, NO and O_2 photolysis, we have not treated this temperature dependence explicitly, but have used cross-sections measured at roughly 230°K for all temperatures. As a result several of our calculated trace species photodissociation rates should be more accurate for the stratosphere then the lower troposphere.

The solar flux is divided into 148 wavelength bins extending from 133.3 nm to 735.0 nm. The size of the individual bins increases from 0.9 nm at lower wavelengths to 10.0 nm in the upper wavelength region. The solar flux at the top of the atmosphere is based on the recommendations of Hudson and Reed (1979). The solar zenith angle is varied with time for diurnal calculations and is held fixed for diurnal-averaged calculations at a value corresponding to noon at 30°N at solar equinox.

In order to accurately compute photodissociation rates, it is important to describe radiative processes, such as multiple scattering, in addition to attenuation by gases such as O_2, O_3 and NO_2. Multiple scattering is included in the model using a simplified method that is computationally fast so that it can be used for diurnal calculations. The method is similar to that of Isaksen et al. (1977) in terms of the numerical method but quite different in terms of the physical assumptions. The atmosphere is divided into optically thick layers and each layer can absorb and scatter radiation. The layer is assumed to scatter radiation isotropically with half of the scattered flux going upward and the other half downward at an average zenith angle. The earth's surface is also assumed to scatter isotropically, and a surface albedo of 0.25 is used to approximate the effect of clouds on the upward scattered radiation. Using a high surface albedo and no clouds gives results that are nearly identical to those from dividing the atmosphere into clear and cloudy regimes and averaging the results (the exception being the region below the cloud layer, which is not important for the model applications considered here). For each atmospheric layer there is a contribution to the solar flux density from the direct flux and by the diffuse fluxes incident on the layer from above and from below. The flux density due to the various fluxes together can be much greater (depending on the wavelength and altitude) than the flux density computed considering only gaseous absorption (Luther and Gelinas, 1976; Luther and Wuebbles, 1976).

The effect of clouds on photolysis rates in the lower troposphere is included by multiplying the photolysis rates calculated in the model by a factor which is a function of altitude. The multipliers used are shown in Table 4. These multipliers are based on a subjective analysis of available data on the amount of cloudiness and cloud types in the troposphere (Hoyt, 1976), cloud type altitude, cloud albedo, and cloud absorptivities.

Table 4. Multiplier of tropospheric photolysis rates to account for clouds

Altitude	Multiplier
0	0.7
1	0.7
2	0.7
3	0.75
4	0.83
5	0.83
6	0.97
7	0.97
8	0.97
9	0.98
10	0.99
11 on	1.0

BOUNDARY CONDITIONS

The model allows for either fixed concentrations or a flux condition at the surface as a lower boundary condition. For most of the calculations, six species are assumed to have fixed concentrations (see Table 5), while a surface flux was assigned to the other species. Zero flux was assumed except for those species shown in Table 5. When those species with fixed boundary conditions in Table 5 are given flux boundaries, a flux is determined to give an ambient concentration the same as those in Table 5.

Zero flux is assumed for all species except NO and NO_2 at the upper boundary. NO and NO_2 are assumed to have a very small flux from the mesosphere into the stratosphere.

Water vapor concentrations are fixed in the troposphere and calculated in the stratosphere. Water vapor concentrations in the troposphere are based on 30°N data from Oort and Rasmussen (1971).

Table 5. Boundary conditions

Fixed Mixing Ratios	
N_2O	300. ppmv
CH_4	1.65 ppmv
H_2	0.56 ppmv
CH_3Cl	0.62 ppbv
CO	0.12 ppmv
H_2O	1.69×10^{-2}
Surface Flux (molecules $cm^{-2}s^{-1}$)	
NO	1.60×10^{9}
NO_2	3.30×10^{9}
HNO_3	1.67×10^{9}
HCl	3.67×10^{10}

Sources and Sinks

In addition to sources and sinks from the chemistry and boundary conditions described above, there are additional sinks due to dry and/or wet removal for many species in the model. A source for nitric oxide from cosmic ray dissociation of N_2 is also included based on the results of Nicolet (1974).

Wet removal processes are parameterized by a first-order loss rate. The wet removal of the trace species HNO_3, H_2O_2, HCl, ClO, $ClONO_2$, $ClNO_2$, HNO_4, HOCl, CH_2O and CH_3OOH is assumed to vary with altitude as shown in Table 6. NO_2 is assumed to have a loss rate half the above rate.

Dry deposition rates at the surface are also parameterized by a first-order loss rate as shown in Table 7. These loss rates apply only when a species does not have a fixed surface concentration.

Table 6. Wet removal parameterization

Altitude, km	Loss Rate, sec^{-1}
0	3.86×10^{-6}
1	3.86×10^{-6}
2	3.86×10^{-6}
3	3.86×10^{-6}
4	3.86×10^{-6}
5	3.86×10^{-6}
6	1.93×10^{-6}
7	1.93×10^{-7}
8	9.58×10^{-7}
9	4.78×10^{-7}
10	0

Table 7. Dry deposition rates in the lowest layer (z=0).

Species	Loss Rate (sec^{-1})	Species	Loss Rate (sec^{-1})
$O(^3P)$	1.0×10^{-5}	NO_3	2.0×10^{-5}
O_3	4.0×10^{-6}	N_2O_5	2.0×10^{-5}
NO	1.0×10^{-6}	H_2O	0
NO_2	3.0×10^{-6}	HNO_4	2.0×10^{-5}
N_2O	0	HOCl	2.0×10^{-5}
HNO_3	2.0×10^{-5}	HCO	2.0×10^{-5}
OH	2.0×10^{-5}	CH_2O	1.0×10^{-5}
HO_2	2.0×10^{-5}	CH_3	2.0×10^{-5}
H_2O_2	2.0×10^{-5}	CH_3OOH	2.0×10^{-5}
Cl	2.0×10^{-5}	CH_3O	2.0×10^{-5}
$ClONO_2$	2.0×10^{-5}	CH_3O_2	2.0×10^{-5}
ClO	2.0×10^{-5}	CO	5.0×10^{-7}
CH_4	0	ClO_3	2.0×10^{-5}
H_2	1.0×10^{-7}	OClO	2.0×10^{-5}
CH_3Cl	0	HONO	2.0×10^{-5}
$ClNO_2$	2.0×10^{-5}		
HCl	2.0×10^{-5}		
CCl_4	0		

Other Physical Data

The N_2 and O_2 distributions are fixed based on the U.S. Standard Atmosphere (1976). The temperature distribution, when held fixed, is usually based on the U.S. Standard Atmosphere (1976) data for mid-latitudes.

TEMPERATURE FEEDBACK

Although many calculations with the model are made assuming a constant temperature distribution with time, the capability also exists to determine the temperature explicitly at stratospheric altitudes as a function of time. When this temperature feedback process is included, the temperature profile above 13 km is calculated using a stratospheric radiative transfer model, and the temperature profile is specified at lower altitudes. The model includes solar absorption and long-wave interaction by O_3, H_2O, and CO_2, along with solar absorption by NO_2. The techniques adopted for treating long-wave radiative transfer are the same as those described by Ramanathan (1974). This formulation was chosen because it is computationally efficient, and its accuracy has been demonstrated (Ramanathan, 1974, 1976) by comparison with much more complex models. The effects of and justification for the simplifying assumptions used in the model are discussed by Ramanathan (1976).

A band absorptance formulation is used to treat the 9.6-μm band of O_3 and the fundamental and several hot and isotopic bands of CO_2 in the 15-μm region. An emissivity formulation is used to treat long-wave radiative transfer by H_2O. Solar absorption by O_3 is treated by using the empirical formulation given by Lindzen and Will (1973). The band absorptance formulation by Houghton (1963) is adopted for solar absorption by H_2O, and the band absorptance formulation by Ramanathan and Cess (1974) is adopted for solar absorption by CO_2. The empirical formulation of Luther (1976) is used for solar absorption by NO_2. Solar absorption by O_3 and NO_2 are treated independently because absorption by these species is weak in the region where their absorption bands overlap. Solar radiation scattered from the troposphere is included by assuming an albedo of 0.3. Doppler broadening effects are included for CO_2 and O_3 as described in Appendix B of Ramanathan (1976). The temperature dependences of the band absorptance and band intensity are included in the longwave calculations of CO_2 and O_3.

A single cloud layer is included at 6.5 km with 42% cloud cover as was suggested by Cess (1974). The lapse rate within the troposphere is assumed to be -6.5 K/km, and the temperature at the earth's surface is specified to be 288 K.

DIURNAL AND DIURNAL-AVERAGED MODELING

In addition to the capability for diurnal calculations, we have also developed a fully diurnal-averaged model that is consistent with our diurnal model. The diurnal model is used to generate species profiles for comparison with measurements and for perturbation studies involving short time integrations (e.g., solar eclipse effects). The diurnal-averaged model is used for perturbation and sensitivity studies involving longer time integrations. There is a significant computer time saving in using the diurnal-averaged model for calculations longer than a few model days.

The procedure that is used in developing the fully diurnal-averaged model is also applicable to two-dimensional models. If the continuity equation is averaged over a time period (24 hours in our case) that is very small compared to the time scale of the problem of interest, then one obtains averaged terms of the form $\overline{k_{ij}c_ic_j}$ and $\overline{J_ic_i}$ where c_i is the concentration of species i at time t and altitude z, k_{ij} is the two-body chemical rate coefficient, and J_i is the photodissociations rate coefficient for species i.

We define the diurnal weighting factors $\alpha_{ij}(z)$ and $\beta_i(z)$ by

$$\overline{k_{ij}c_ic_j} = \alpha_{ij}\,\overline{k_{ij}}\;\overline{c_i}\;\overline{c_j}$$

and

$$\overline{J_ic_i} = \beta_i\,\overline{J_i}\;\overline{c_i}\ .$$

Since k_{ij} is defined and is independent of time, we have

$$\alpha_{ij} = \overline{c_i c_j} \; / \; \overline{c_i}\,\overline{c_j}$$

and

$$\beta_i = \overline{J_i c_i} \; / \; \overline{J_i}\,\overline{c_i} \; .$$

The computation of photodissociation rates can be an expensive part of stratospheric model calculations, hence evaluation of J_i's in the diurnal-averaged model can be expensive. If we define β_i by

$$\beta_i = \overline{J_i c_i} \; / \; (J_i^{noon}\,\overline{c_i}) \; ,$$

then the computation in the *diurnal-averaged* model is greatly simplified. The diurnal model is used to determine $\overline{c_i c_j}$, $\overline{J_i c_i}$, $\overline{c_i}$, $\overline{c_j}$, and J_i^{noon} so that α_{ij} and β_i can be obtained for every chemical and photochemical reaction in the model.

A basic assumption in this approach is that α_{ij} and β_i are relatively insensitive to changes in c_i and c_j. This is generally the case, however, because the α_{ij} and β_i primarily represent functional *weighting* factors which are sensitive to the functional shape of the diurnal variations in c_i and c_j and not to changes in the absolute magnitude of c_i and c_j. So long as there is no drastic change to stratospheric ozone, there should be very little change in the diurnal functional shape of all the species. If there are significant changes, the diurnal model can be used to reevaluate the α_{ij} and β_i and iterate this averaging process.

REFERENCES

Bass, A. M., L. C. Glasgow, C. Miller, J. P. Jesson, and D. L. Filkin, "Temperature Dependent Absorption Cross Sections for Formaldehyde (CH_2O): The Effect of Formaldehyde on Stratospheric Chlorine Chemistry," in Proceedings of the NATO Advanced Institute on Atmospheric Ozone, Portugal, 1980, available as U.S. Dept. of Transportation Report FAA-EE-80-20, 1980.

Cess, R. D., "Radiative Transfer Due to Atmospheric Water Vapor: Global Considerations of the Earth's Energy Balance," J. Quant. Spectrosc. Radiat. Transfer, 14, 861-871, 1974.

Chang, J. S., A. C. Hindmarsh, and N. K. Madsen, "Simulation of Chemical Kinetics Transport in the Stratosphere in Stiff Differential Systems," edited by R. A. Willoughby, Plenum Publishing Corp., New York, p. 51 ff, 1974.

Chang, J. S., "Simulations, Perturbations, and Interpretations," in Proceedings of the 3rd CIAP Conference, U.S. Dept. of Transportation, Cambridge, MA, Report DOT-TSC-OST-74-15, 330-341, 1974.

Chang, J. S., J. R. Barker, J. E. Davenport, and D. M. Golden, "Chlorine Nitrate Photolysis by a New Technique: Very Low Pressure Photolysis," Chem. Phys. Lett., 60, 385-390, 1979

Cox, R. A, "Kinetics of HO_2 Radical Reactions of Atmospheric Interest," presented at the WMO Symposium on the Geophysical Aspects and Consequences of Change in the Composition of the Stratosphere, Toronto, June 26-30, 1978, WMO No. 511, 1978.

Davidson, J. A., H. I. Schiff, T. J. Brown, and C. J. Howard, "Temperature Dependence of the Rate Constants for Reactions of $O(^1D)$ Atoms with a Number of Halocarbons," J. Chem. Phys., 69, 4277-4279, 1978.

DeGraff, B. A., and J. G. Calvert, "A Study of the Primary Processes in CH_2O and CD_2O Photolysis, J. Amer. Chem. Soc., 89, 2247-2253, 1967.

Duewer, W. H., D. J. Wuebbles, H. W. Ellsaesser, and J. S. Chang, "NO_x Catalytic Ozone Destruction: Sensitivity to Rate Coefficients," J. Geophys. Res., 82, 935-942, 1977.

Frederick, J. E. and R. D. Hudson, "Predissociation of Nitric Oxide in the Mesosphere and Stratosphere," J. Atmos. Sci., 36, 737-745, 1979.

Graham, R. A., A. M. Winer and J. N. Pitts, Jr., "Pressure and Temperature Dependence of the Unimolecular Decomposition of NO_2NO_2," J. Chem. Phys., 68, 4505-4510, 1978.

Hampson, R. F., "Chemical Kinetic and Photochemical Data Sheets for Atmospheric Reactions," U.S. Dept. of Transportation Report No. FAA-EE-80-17, 1980.

Houghton, J. T., "The Absorption of Solar Infrared Radiation by the Lower Stratosphere," Quart. J. Roy. Meteorol. Soc., 89, 319-331, 1963.

Hoyt, D. V., "The Radiation and Energy Budget of the Earth Using Both Ground Based and Satellite-Derived Values of Total Cloud Cover," NOAA TR ERL 362-ARL 4, 1976.

Hubrich, C., C. Zetzach and F. Stuhl, "Absorptionspektren von Halogenierten Methanen von 275 bis 160 nm bei Temperaturen von 298 und 208 K," Ber. Bunenges Phys. Chem, 81, p. 437-442, 1977.

Hubrich, C. and F. Stuhl, "The Ultraviolet Absorption of Some Halogenated Methanes and Ethanes of Atmospheric Interest," J. Photochem., 12, 93-107, 1980.

Hudson, R. D. and S. H. Mahle, "Photodissociation Rates of Molecular Oxygen in the Mesosphere and Lower Thermosphere," J. Geophys. Res., 77, 2902-2914, 1972.

Hudson, R. D. and E. I. Reed, "The Stratosphere: Present and Future," NASA Reference Publication 1049, 1979.

Isaksen, I. S. A., K. M. Midtbo, J. Sunde, and P. J. Crutzen, "A Simplified Method to Include Molecular Multiple Scattering and Reflection in Calculations of Photon Fluxes and Photodissociation Rates," Geophysica Norwegica, 31, 11-26, 1977.

Lindzen, R. S. and D. I. Will, "An Analytical Formula for Heating Due to Ozone Absorption," J. Atmos. Sci., 30, 513-515, 1973.

Luther, F. M., "A Parameterization of Solar Absorption by Nitrogen Dioxide," J. Appl. Meteorol., 15, 479-481, 1976.

Luther, F. M. and R. J. Gelinas, "Effect of Molecular Multiple Scattering and Surface Albedo on Atmospheric Photodissociation Rates," J. Geophys. Res., 81, 1125-1132, 1976.

Luther, F. M. and D. J. Wuebbles, "Photodissociation Rate Calculations," Report UCRL-78911, Lawrence Livermore Laboratory, Livermore, CA, 1976.

Luther, F. M., J. S. Chang, W. H. Duewer, J. E. Penner, R. L. Tarp, and D. J. Wuebbles, "Potential Environmental Effects of Aircraft Emissions," Lawrence Livermore National Laboratory Report UCRL-52861, 1979.

Molina, L. T. and M. J. Molina, "Ultraviolet Absorption Cross Sections of HO_2NO_2 Vapor," presented at the 14th Informal Conference on Photochemistry, Newport Beach, CA, March 30-April 3, 1980, also U.S. Dept. of Transportation Report FAA-EE-80-7, 1980.

Moortgat, G. K., and P. Warneck, "CO and H_2 Quantum Yields in the Photodecomposition of Formaldehyde in Air," J. Chem. Phys., 70, 3639-3651, 1979.

NASA Panel for Data Evaluation, "Chemical Kinetic and Photochemical Data for Use in Stratospheric Modeling," Jet Propulsion Laboratory, Publication 79-27, 1979.

NASA Panel for Data Evaluation, "Chemical Kinetic and Photochemical Data for Use in Stratospheric Modeling, Evaluation Number 4," Jet Propulsion Laboratory Publication 81-3, 1981.

National Research Council, "Halocarbons: Effects on Atmospheric Ozone," National Academy of Sciences, Washington, D.C., 1976.

NBS Special Publication 513, "Reaction Rate and Photochemical Data for Atmospheric Chemistry -- 1977," R. F. Hampson, Jr. and D. Garvin (eds.), National Bureau of Standards, Washington, D. C. 1978.

Nicolet, M., "On the Production of Nitric Oxide by Cosmic Rays in the Mesosphere and Stratosphere," Aeronomica Acta-A, No. 134, Institut D'Aeronomie Spatiale de Belgique, Brussels, 1974.

Oort, A. H. and E. M. Rasmussen, "Atmospheric Circulation Statistics," NOAA Professional Paper 5, 1971.

Pitts, J. N., Jr., H. L. Sandoval, and R. Atkinson, "Relative Rate Constants for the Reaction of $O(^1D)$ Atoms with Fluorocarbons and N_2O," Chem. Phys. Lett., 29, p. 31-34, 1974.

Ramanathan, V., "A Simplified Stratospheric Radiative Transfer Model: Theoretical Estimates of the Thermal Structure of the Basic and Perturbed Stratosphere," paper presented at the Second International Conference on the Environmental Impact of Aerospace Operations in the High Atmosphere, American Meteorological Society/American Institute of Aeronautics and Astronautics, San Diego, Calif., July 8-10, 1974.

Ramanathan, V., "Radiative Transfer Within the Earth's Troposphere and Stratosphere: A Simplified Radiative-Convective Model," J. Atmos. Sci., 33, 1330-1346, 1976.

Ramanathan, V. and R. D. Cess, "Radiative Transfer Within the Mesospheres of Venus and Mars," Astrophys. J., 188, 407-416, 1974.

Thompson, B. A., P. Harteck and R. R. Reeves, Jr., "Ultraviolet Absorption Coefficients of CO_2, CO, O_2, H_2O, N_2O, NH_3, NO, SO_2, and CH_4 Between 1850 and 4000 A." J. Geophys. Res., 68, 6431-6436, 1963.

U.S. Standard Atmosphere, 1976, NOAA-S/T 76-1562, U.S. Government Printing Office, Washington, D.C., 1976.

Watson, R. T., "Chemical Kinetics Data Survey VIII. Rate Constants of ClO_x of Atmospheric Interest," NBSIR 74-516, National Bureau of Standards, Washington, D. C., 1974.

DJW:clm:00451I

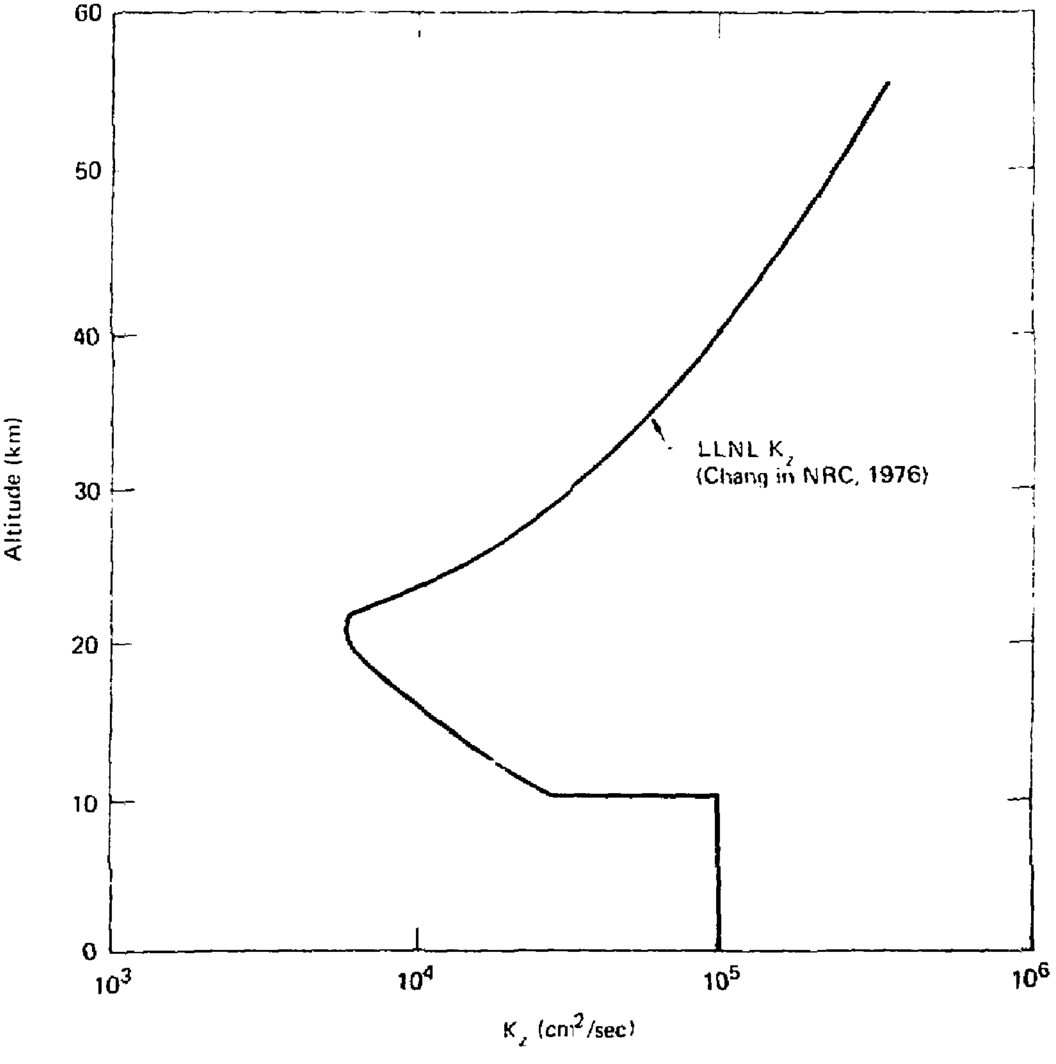

Figure 1. Diffusive transport coefficient primarily used in LLNL 1-D model.